

Rotation Table Experiments and Write-up

Janet Peifer

February 28, 2019

Contents

| | | |
|----------|---|-----------|
| 1 | Introduction | 3 |
| 2 | Rotation Table | 4 |
| 2.1 | Design | 4 |
| 2.2 | Materials | 4 |
| 2.3 | Set-up | 4 |
| 3 | Mathematical Preliminaries | 5 |
| 4 | Taylor-Proudman Columns | 7 |
| 4.1 | Theory | 7 |
| 4.2 | Experiments | 8 |
| 4.3 | Results | 11 |
| 4.4 | Conclusions | 11 |
| 5 | Rossby Waves | 11 |
| 5.1 | Theory | 11 |
| 5.2 | Experiment | 12 |
| 5.3 | Results | 12 |
| 5.4 | Conclusions | 14 |
| 6 | Ekman Layer | 14 |
| 6.1 | Theory | 14 |
| 6.2 | Experiment | 16 |
| 6.3 | Results | 16 |
| 6.4 | Conclusions | 16 |
| 7 | General Conclusions and Comments | 19 |

8 Bibliography **19**

9 Risk Assessment **20**



Figure 1: The Coriolis Platform at Laboratoire des Ecoulements Géophysiques et Industriels (LEGI) in Grenoble, France. It is 13m in diameter and holds 1m depth of liquid (Gostiaux).

1 Introduction

IN the field of astrophysical and geophysical flows, studies on rotating fluids have high prominence as researchers seek to understand flows on rotating planets. The study of such flows has lead to a great deal of understanding of rotating fluids in a variety of limits. In the rapidly rotating limit, Taylor-Proudman "Theorem", Rossby waves, and Ekman Layers become important.

Experimental results are used to support and visualize mathematical theories. Rotation tables have come into popularity for the experimental study of geophysical and astrophysical flows on a basic and advanced level. There are massive rotation tables, the largest being the Coriolis platform in Grenoble (see Figure 1) and the most basic being available to anyone with a record machine (see Figure 2)! The robust nature of these flows and the mathematics used to describe them is evident as they can be proven in even the most basic experiments.

This report will examine the relationship between the mathematics and experimental observation. First, the mathematics underlying all of the following experiments will be described. Then, the rotation table will be introduced. In the latter sections, the mathematics of each phenomena will be examined and the limits within which the maths hold true identified. Then, experimental procedures and observations are put forth. Concluding remarks will include the success of the experiments to achieve the reality of the maths and reasons for any success, or lack thereof.



Figure 2: An experimental set-up using a record player as a rotation table from Spinlab at UCLA (ucla spinlab, 2014).

2 Rotation Table

2.1 Design

The rotation table is a plate of wood rotated clockwise by motor (see Figure 3).

2.2 Materials

1. Cylindrical bowl
2. Square bowl
3. Food dye
4. Go Pro
5. Go Pro stand
6. Power supply
7. Electrical cables
8. Water

2.3 Set-up

The following procedure was used to set-up and operate the rotation table:

1. Set rotation table kit on flat surface and open the large end (see Figure 3).



Figure 3: The rotation table working parts. Two size of spinners are used to varying speeds. the smaller wheel rotates slower than the larger one.

2. Ensure that the belt is around the larger wheel for fastest rotation (see Figure 3).
3. Reattach the kit top, leaving the leads to the motor outside.
4. Connect the power supply to the motor by connecting the negative cable to the brown lead and the positive cable to the blue lead.
5. Place the bowl and topography (determined by the requirements of the respective experiment) on the rotation table and fill with desired amount of water.
6. Perform any other preparations specific to the desired experiment.
7. Turn on the power supply and set it to desired voltage (generally 12.0 V (Kreczak, 2018))
8. To begin rotation, press the 'Output' button on the power supply.

3 Mathematical Preliminaries

The mathematical basis for these experiments relies on rapidly rotating geo-physical flows. For further detail, suggested reading includes Bokhove (2018) and Vallis (2006). Geophysical flows with velocity \mathbf{u} , density ρ , pressure

p , and acted on by body forces \mathbf{F} , are often described beginning with the Navier-Stokes momentum equation with incompressibility:

$$\frac{D\mathbf{u}}{Dt} = -\frac{1}{\rho} \nabla p + \mathbf{F}, \quad (1)$$

and

$$\nabla \cdot \mathbf{u} = 0. \quad (2)$$

Additionally, the Boussinesq approximation is made in large-scale oceanic and atmospheric flows where fluid density varies ± 2 percent. In this approximation, density is considered a constant for all terms except for gravity, such that $\mathbf{F} = \rho\mathbf{g}$:

$$\rho \frac{D\mathbf{u}}{Dt} = \nabla p - \rho\mathbf{g}. \quad (3)$$

Additionally, the influence of rotation on these essential equations is influential to the phenomena explored later in this report. In a rotating frame, two terms come into play: the coriolis force and the centrifugal force, neither of which are true forces. Of the two, the coriolis force is much more relevant to this report. The coriolis force is $2\Omega \times \mathbf{u}$ where Ω is the rotation velocity around the rotation axis. This force deflects horizontally moving flows to the left or right of their path. This addition makes eq(2) become:

$$\frac{D\mathbf{u}}{Dt} + 2\Omega \times \mathbf{u} = \frac{-1}{\bar{\rho}} \nabla p - \frac{\rho g}{\bar{\rho}} \mathbf{e}_z, \quad (4)$$

where $\bar{\rho}$ is the average density. With this consideration and further manipulations, some more physically meaningful themes and useful numbers arise.

In the determination of rapid rotation opposed to slow rotation, a useful value arises. By undimensionalizing eq(4), in terms of characteristic length L and velocity U , the relationship between these values and the coriolis force becomes apparent. The Rossby number, a dimensionless number which compares the ratio of inertial force to Coriolis force, is used to mark the range of rapid rotation. Thus,

$$Ro = \frac{U}{f_o L}, \quad (5)$$

where $f_o = 2\Omega$ is the Coriolis term. When the $Ro \ll 1$, then geostrophic balance holds.

Geostrophic balance is a key concept in large scale geophysical flows. It is defined as the result of the implementation of $Ro \ll 1$ to the Boussinesq equations in a rotating frame (eq 4):

$$2\Omega \times \mathbf{u} = \frac{-1}{\bar{\rho}} \nabla p. \quad (6)$$

Looking at equation (6), it is clear that geostrophic balance occurs when the coriolis term is balanced with the pressure gradient, and their magnitude is significantly larger than the other terms addressed in equation (4).

These themes and concepts will shape the background for Taylor-Proudman Columns, Rossby Waves, and Ekman Layers.

4 Taylor-Proudman Columns

4.1 Theory

Taylor-Proudman Columns are the physical representation of the Taylor-Proudman 'Theorem', which says that a rapidly rotating fluid will have velocity independent of the rotation axis. This theorem derives from the Navier-Stokes momentum equation for a fluid of constant density:

$$\frac{D\mathbf{u}}{Dt} + 2\boldsymbol{\Omega} \times \mathbf{u} = \frac{-1}{\rho} \nabla p - \nabla \Phi_c + \mathbf{F} + \nu \nabla^2 \mathbf{u}, \quad (7)$$

where \mathbf{u} is fluid velocity, $\boldsymbol{\Omega}$ is rotation velocity, ρ is density, p is pressure, Φ_c is the centrifugal potential, \mathbf{F} represents body forces, and ν is viscosity.

Then, considering an inviscid fluid ($\nu = 0$) where gravity is the only body force, thus $f = g = \nabla \Phi$. Additionally, in the rapidly rotating limit, such that $Ro \ll 1$, the Coriolis term is significantly larger than the material derivative, $\boldsymbol{\Omega} \times \mathbf{u} \gg \frac{D\mathbf{u}}{Dt}$. The equation (7) can then be written as:

$$2\boldsymbol{\Omega} \times \mathbf{u} = \nabla X, \quad (8)$$

where $X = \frac{-p}{\rho} - \Phi_c + \Phi$.

Now taking the cross product:

$$\nabla \times 2\boldsymbol{\Omega} \times \mathbf{u} = \nabla \times \nabla X. \quad (9)$$

Using vector identities:

$$\nabla \times 2\nabla X, \quad (10)$$

$$2\boldsymbol{\Omega}(\nabla \cdot \mathbf{u} - 2\mathbf{u} \cdot \nabla \boldsymbol{\Omega}) + 2\mathbf{u} \cdot \nabla \boldsymbol{\Omega} - 2\boldsymbol{\Omega} \cdot \nabla \mathbf{u} = 0. \quad (11)$$

Application of incompressibility and the system's characteristics, it is found that:

$$\boldsymbol{\Omega} \times \nabla \mathbf{u} = 0, \quad (12)$$

which states that velocity is independent of the axis of rotation. Thus, the Taylor-Proudman "Theorem" is derived.

Due to this derivation, it is expected that if there is an obstacle to a flow at any vertical position in a plane rotating about the z-axis, that the flow will avoid the vertical area above and below the obstacle. Instances of this are called Taylor Columns .

4.2 Experiments

To visualize the Taylor-Proudman "Theorem", a small obstacle is placed at the bottom of a rotating table and the fluid path around it is observed. The round table will be used. The additional materials needed for this experiment include:

1. Puck of cylindrical shape, significantly smaller than the bowl
2. Pipette

The experimental procedure is:

1. Set-up rotation table (Steps 1-5 from section 2.3).
2. Screw GoPro stand into the rotation table.
3. Screw the GoPro onto its backboard and attach backboard to the stand such that the backboard is level with the top of the bowl.
4. Turn on GoPro.
5. Place puck underneath the lens of the GoPro, apx 10cm from the wall of the bowl.
6. Continue rotation table set-up Steps 6,7 from section 2.3.
7. Let the table run-up for a 15 minute minimum.
8. Meanwhile, mix a cup of water with some suitably dark dye
9. After 15 minutes, begin GoPro video.
10. Get a pipette full of dyed water and squirt it into the tank in a line directly in front of the camera's path (see Figure 4).
11. Using the knob labeled "fine" to increase the voltage to 12.2 V (Kreczack, 2018).
12. Allow the table to rotate until the dye is barely visible.
13. Turn off the power supply and the GoPro



Figure 4: Location for inserting dye into the rotation table for the Taylor column experiment.



Figure 5: Proof of Taylor Proudman

4.3 Results

The completion of this experiment was met with success. The Taylor Column appeared as expected in the form of the dye diverting from its direct path as it does not pass over the puck (see Figure 5).

4.4 Conclusions

Overall, experimental results back up the mathematical theories expressed in section 4.1. Though the dye did cover small portions of the space directly over the puck, it was very evident from observation that the dye diverted around the vertical space of the puck, as predicted by the Taylor-Proudman "Theorem".

5 Rossby Waves

5.1 Theory

Rossby waves is a phenomena wherein the divergence of fluid parcels from their original course causes a change in vorticity creating a moving wave. Within the Boussinesq approximation, and geostrophic balance, as similarly required for Taylor-Proudman Columns, Rossby waves too occur. Considering, as in Bokhove (2018), $\rho = \rho(z)$ and no forcing, $\mathbf{F} = 0$, total vorticity can be defined as,

$$\mathbf{q} = \mathbf{f} + \boldsymbol{\omega}, \quad (13)$$

where \mathbf{f} is planetary vorticity and $\boldsymbol{\omega} = \frac{\partial v}{\partial x} - \frac{\partial u}{\partial y}$ is relative vorticity.

The vorticity equation under the Boussinesq approximation is,

$$\frac{D\mathbf{q}}{Dt} = (\mathbf{q} \cdot \nabla) \mathbf{u}. \quad (14)$$

However, using the considerations stated above, this becomes, $\frac{D\mathbf{q}}{Dt} = 0$. This indicates that the scalar of the absolute vorticity is materially conserved. Thus, when a fluid parcel is displaced along y axis, and the planetary vorticity changes, the relative vorticity must compensate. This causes the fluid parcels to spin and drive them back toward their original location. Due to the spin, the parcels are then moved along the x axis as well. Figure 6 describes the process for a rotation eastward (to the right) about the z axis, which would be coming out of the page.

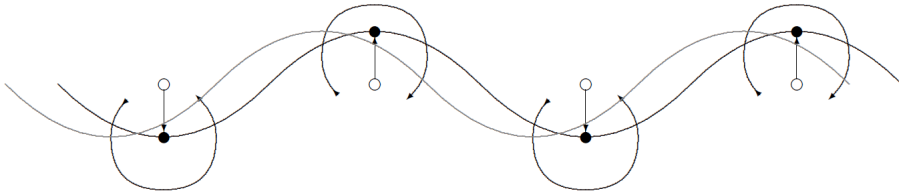


Figure 6: The propagation of a Rossby wave: As fluid parcels are displaced (white circles), their relative vorticity changes to conserve total vorticity. If displaced northward (up page), vorticity decreases, causing clockwise rotation and vice versa for southward displacement. The parcel is drawn back toward its original path (black line), but due to the change in relative vorticity, the entire wave propagates westward (left page). (Bokhove, 2018).

5.2 Experiment

In order to visualize Rossby waves, a sloped topography is used to cause a variation in vorticity, such that at the shallow end the vorticity is increased from the deep end, mimicking the variation found moving north and south along a planet. The square bowl will be used. The additional materials required are:

1. Square sloped topography (45 degree slope for this case)
2. Ice cube of dyed water

The procedure, influenced by the experimental design of Illari and Marshall, is as follows:

1. Set-up tank as described in section 2.1 steps 1-7, making sure to put the topography into the bowl and filling with water close to the top of the topography.
2. Place an ice cube toward the shallower end of the tank.
3. Record and observe until dye has diffused past visibility or the ice cube reaches the western wall.

5.3 Results

The experiment showed a wave propagated westward (see Figure 7) as predicted by the theory explained in Section 5.2.

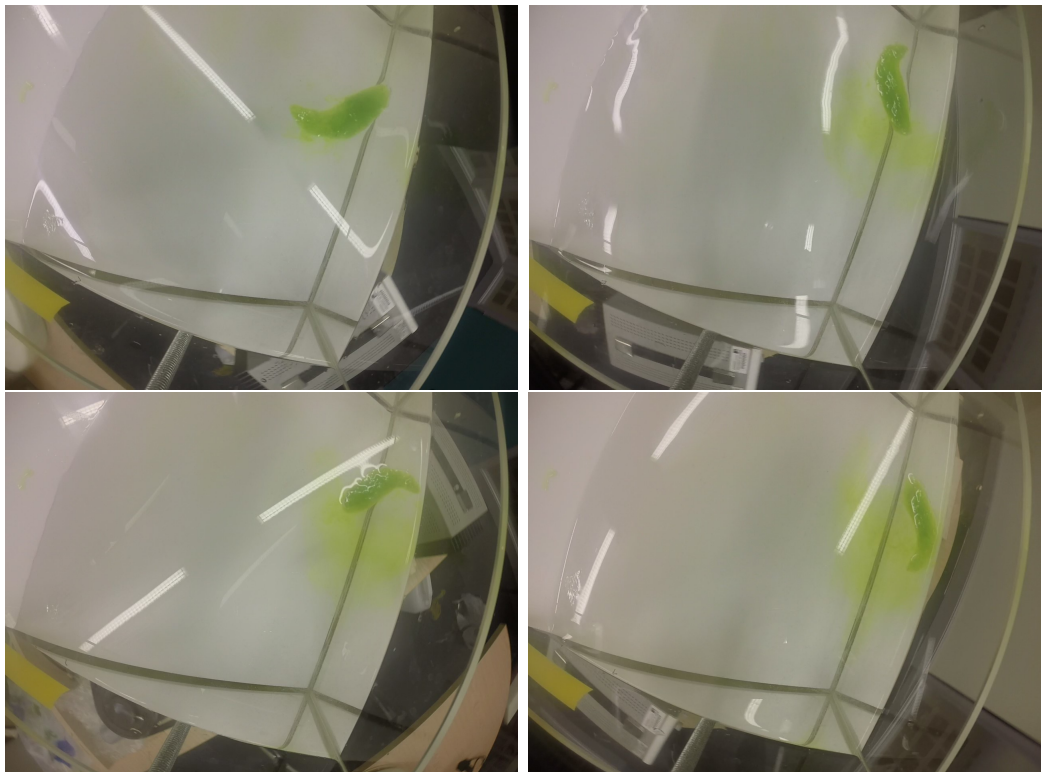


Figure 7: Orientation in each photo is such that left is North, top is East, right is South, and bottom is West. From left top to right bottom: Images taken approximately 10 seconds apart, showing the progression of the wave and ice cube westward.

5.4 Conclusions

The clockwise rotation of the table, would lead us to expect eastward propagation of the wave. To this end, the experiment was marginally successful. The dye was not dark enough, and the unsymmetrical shape of the ice cube may have caused odd diffusion patterns. However, the basic path of the fluid follows the trajectory predicted by the theory of Rossby waves.

6 Ekman Layer

6.1 Theory

Large-scale flows like atmospheric and oceanic flows are close to geostrophic balance, where, as shown in Section 3, the flow is independent of z . represent geostrophic flows flows where $v_g = v(x, y, z)$ and $u_g = u(x, y, z)$ far away from boundaries where other forces, such as friction become significant, the momentum equations become:

$$-2\Omega v_g = \frac{-1}{\rho} \frac{\partial p}{\partial x}, \quad (15)$$

$$2\Omega u_g = \frac{-1}{\rho} \frac{\partial p}{\partial y}. \quad (16)$$

Equations (15) and (16) apply close to boundary layers, where, for instance, fluids meet a solid surface, factors which are able to be neglected in the middle of the flow become important. In oceanic flows, the region where friction becomes important, is called the Ekman Layer.

The Taylor-Proudman "Theorem" says that flows in geostrophic balance will be independent of the axis of rotation. However, boundary conditions insist that there be a no-slip condition where the flow meets a rigid surface, thus $\rightarrow 0$ and $v \rightarrow 0$ as $z \rightarrow 0$. To allow for this change, turbulent diffusion is allowed in the boundary layer. Following the derivation in Bokhove (2018) the geostrophic balance can be modified to,

$$-2\Omega v = \frac{-1}{\rho} \frac{\partial p}{\partial x} + \nu \frac{\partial^2 u}{\partial z^2}, \quad (17)$$

and

$$2\Omega u = \frac{-1}{\rho} \frac{\partial p}{\partial y} + \nu \frac{\partial^2 v}{\partial z^2}. \quad (18)$$

Using eq (15) and (16), eq(13) and (14) can be rewritten as,

$$\frac{\partial^2 u}{\partial z^2} = \frac{2\Omega}{\nu} (v_g - v), \quad (19)$$

and

$$\frac{\partial^2 v}{\partial z^2} = \frac{2\Omega}{\nu}(u - u_g). \quad (20)$$

The solution must conform to boundary conditions $u, v = 0$ at $z = 0$ and $(u, v) \rightarrow (u_g, v_g)$ as $z \rightarrow \infty$. To solve, $\Upsilon(x, y, z) = u + iv$, finding,

$$\frac{\partial^2 \Upsilon}{\partial z^2} = \frac{2\Omega}{\nu}(\Upsilon - u_g + iv_g), \quad (21)$$

such that Υ meets the boundary conditions. This forms a differential equation entirely in z . Therefore, a solution exists with particular integral $\Upsilon = u_g + iv_g$ and complementary function $\Upsilon = a(x, y)e^{kx}$. Discarding positive real roots of k to avoid exponential growth, the horizontal wavenumber becomes:

$$k = \frac{-(1+i)}{L}, \quad (22)$$

$$L = \sqrt{\frac{\nu}{\Omega}}. \quad (23)$$

Thus,

$$\Upsilon = u_g + iv_g + a(x, y)e^{\frac{-(1+i)z}{L}}. \quad (24)$$

Consider boundary conditions such that Υ , $a = -(u_g + iv_g)$ and,

$$\Upsilon = (u_g + iv_g)(1 - e^{\frac{-(1+i)z}{L}}). \quad (25)$$

Then finding only the real solutions,

$$u(x, y, z) = u_g(x, y)\left(1 - e^{\frac{-z}{L}} \cos\left(\frac{z}{L}\right)\right) - v_g(x, y)e^{\frac{-z}{L}} \sin\left(\frac{z}{L}\right), \quad (26)$$

and

$$v(x, y, z) = v_g(x, y)\left(1 - e^{\frac{-z}{L}}\right). \quad (27)$$

Thus, it is seen that in these Ekman Layers, velocity becomes dependent on vertical position as well as horizontal position. The shift from vertically independent to vertically dependent flows creates the Ekman. Based on these findings, it is expected that at slower rotation, flows near a boundary will move inward and at faster rotations, flows will move outward. By decreasing the rotation speed, a pressure gradient develops due to geostrophic flow, such that pressure is lower in the center than the walls of the bowl. This causes the flow to move radially inward. Rotation rate can then be increased, having the opposite effect.

6.2 Experiment

To visualize Ekman Layers, it is possible to vary the rotation speed of a rotation table and see the various ways flow at the boundary layer behaves. The round bowl will be used. No additional materials are needed for this experiment.

The experimental procedure, influenced by the experimental design of Illari and Marshall, is:

1. Set-up the rotation table following steps 1-7 of section 2.1.
2. Spin-up the table at 12.0 V for at least 15 minutes.
3. Meanwhile, mix dye with water.
4. After 15 minutes, insert dye into the water at 3 points (see Figure 8).
5. Immediately turn down rotation to approximately 8.0 V.
6. After about 30 seconds, increase the voltage to about 10.0 V. Be sure to make some motion within the video frame to indicate the switch for viewers of the video.
7. Turn off power supply output when dye is no longer visible or suitable video is recorded.

6.3 Results

The experiment showed some indication of movement inward during slowed rotation and slight outward movement of the dye during increased rotation speed. Figure 9 shows the dye before change in rotation speed, during slow rotation, and during increased rotation speed.

6.4 Conclusions

The experiment did not prove to be particularly successful at showing the behavior proposed by the theory as described. Though the dye did indicate the general movement as expected, it became difficult to see the location of the dye as rotation continued, especially in the video. This is likely due to the diffusion of the dye over time and mixing increased by the changes in rotation speed.



Figure 8: Triangular arrangement of the dye within the bowl for Ekman Layer experiment.

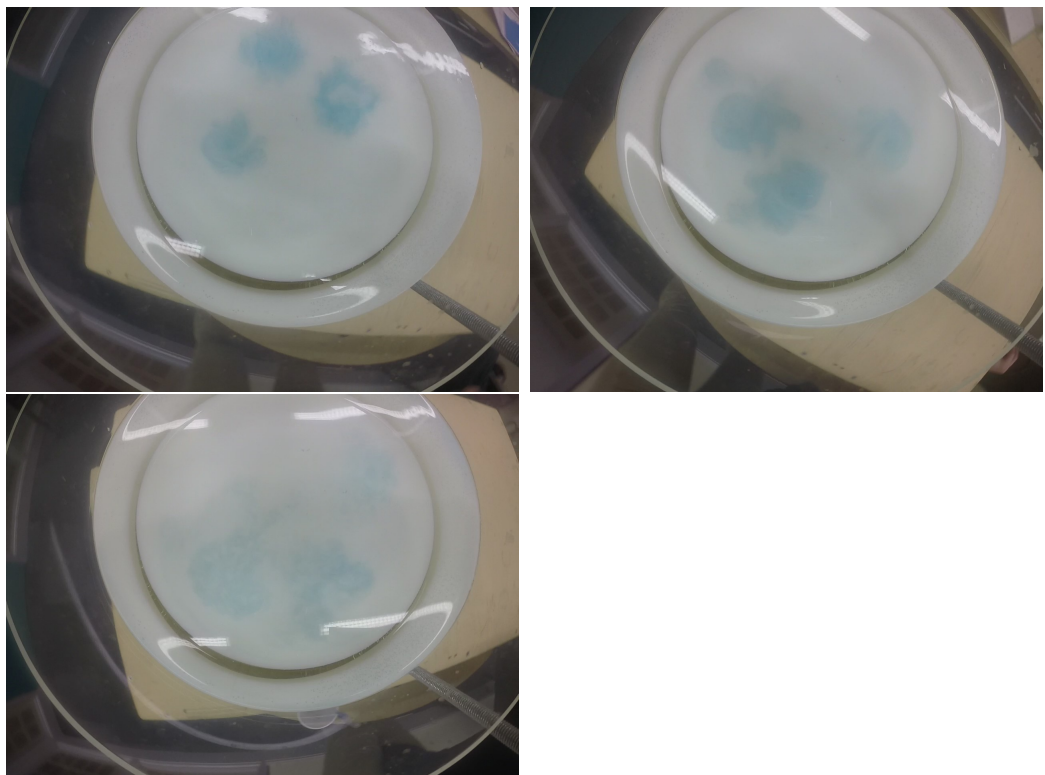


Figure 9: (Top left) At time =15min, the placement of dye after run-up. (Top right) At time= 15min 10s, the position of the dye when voltage was reduced to 8.0 V. (Bottom left) At time= 15min 45s, the position of the dye when voltage was again increased to 10.0 V.

7 General Conclusions and Comments

Overall, these experiments, demonstrate the phenomena explained above: Taylor-Proudman columns, Rossby waves, and Ekman layers. The individual experiments were met with varying success, each having their own difficulties. However, the end results showed the results as expected, as well as was possible with limited materials (i.e. lack of ice cube tray). Improvements could be made with deeper tanks, like that used by the ucla spinlab (2014) which better mimic the atmospheric scale. Additionally, improved lighting and GoPro positioning would result in better images for analysis and demonstration.

Overall, performing these experiments and writing this report has been a good introduction to experimental mathematics and the workings of the rotation table. It is particularly applicable to my own PhD project which will involve advanced understanding of the rotation table as applied to an experiment on rotating convection. By performing these procedures, I have become familiar with the specifics of this rotation table and the experimental methods involved with it. Additionally, the mathematical concepts described and applied in this paper are part of a solid foundation in large-scale, rapidly rotating fluid dynamics which will be applicable to my understanding of the mathematical models will use to describe the behavior of rotating convection with phase change. Another purpose of the description of these procedures is for the demonstration of mathematical concepts in an exciting and accessible way for public outreach events.

8 Bibliography

- Bokhove, O. 2018. Lecture notes distributed in MATH 5458 Advanced Geophysical Fluid Dynamics. 24 February 2019. University of Leeds
- Gostiaux, L. *The Coriolis Platform*. [Online]. [Accessed 19 Feb 2019]. Available from:louis.gostiaux.fr/
- Illari, L. and Marshall, J. *Rossby Waves: Tank- How To (Ice Cubes)*. [Online]. [Accessed 19 Feb 2019]. Available from: weathertank.mit.edu/
- Illari, L. and Marshall, J. *Ekman Layers: Tank- How To*. [Online]. [Accessed 19 Feb 2019]. Available from: weathertank.mit.edu/
- ucla spinlab. 2014. *Record Player Fluid Dynamics: A Taylor Column Experiment*. [Online]. [Accessed 19 Feb 2019]. Available from: <https://www.youtube.com/watch?v=7GGfsW7gOLI> .
- Kreczak, H. 2018. Conversation with Janet Peifer. 30 November.

Vallis, G. K. 2006. *Atmospheric and Oceanic Fluid Dynamics*. Cambridge University Press, 745 pp.

9 Risk Assessment

Full form available: <http://wsh.leeds.ac.uk/info/209/forms/132/forms>

Health and safety services

General risk assessment

| HAZARD AND RELATED ACTIVITIES | PERSONS AT RISK | POSSIBLE OUTCOME | RISK RATING BEFORE CONTROLS (LxS) | EXISTING CONTROLS | RISK RATING AFTER CURRENT CONTROLS (LxS) | FURTHER CONTROLS REQUIRED? | RISK RATING AFTER ADDITIONAL CONTROLS (LxS) |
|---|---|--|-----------------------------------|--|--|----------------------------|---|
| e.g. trip, falling objects, fire, explosion, noise, violence etc. | e.g. Employees, Customers, Contractors, Members of the public | | | e.g. Guards, Safe Systems of Work, Training, Instruction, Authorised Users, Competent Persons, Personal Protective Equipment (PPE) | | | |
| <u>Lifting and transporting kit</u> | <u>Students</u> | <u>Lifting caused injuries and dangers due to possible broken equipment and glass</u> | <u>3x3=9</u> | <u>Corrected and controlled use of handling</u> | <u>2x3=6</u> | | |
| <u>Spillage</u> | <u>Staff, Students, general public</u> | <u>Split water could prove a slipping hazard</u> | <u>3x2=6</u> | <u>Water transported very carefully and spillages promptly marked and cleaned</u> | <u>2x2=4</u> | | |
| <u>Moving parts</u> | <u>Staff and students</u> | <u>Fingers, hair or clothing caught on moving belt</u> | <u>3x2=6</u> | <u>Ensure kit properly covered and precautions taken with loose clothing or hair</u> | <u>1x2=2</u> | | |
| <u>Electrocution</u> | <u>Staff and Students</u> | <u>Combination of water and electrical equipment increases chance of electrocution</u> | <u>3x4=12</u> | <u>All wires and electrical parts covered within kit and careful use of water around equipment</u> | <u>2x4=8</u> | | |